

# INTERNATIONAL SOCIETY FOR SOIL MECHANICS AND GEOTECHNICAL ENGINEERING



*This paper was downloaded from the Online Library of the International Society for Soil Mechanics and Geotechnical Engineering (ISSMGE). The library is available here:*

<https://www.issmge.org/publications/online-library>

*This is an open-access database that archives thousands of papers published under the Auspices of the ISSMGE and maintained by the Innovation and Development Committee of ISSMGE.*

# Effects of shear stress history on yielding of dense Toyoura sand in $p'$ -constant shear plane

Les effets de l'histoire de sollicitation en contraintes de cisaillement sur l'écoulement plastique du sable de Toyoura dense a contrainte moyenne effective constante

J. Kuwano

Department of Civil Engineering, Tokyo Institute of Technology, Tokyo, Japan

T. Nakada

Obayashi Corporation, formerly Tokyo Institute of Technology, Tokyo, Japan

## ABSTRACT

Effects of shear stress history on yielding characteristics of dense Toyoura sand are investigated. The yielding behavior in  $p'$ -constant plane is characterized, especially at small strain level, by introducing two sub yield surfaces  $Y_1$  and  $Y_2$  inside the conventional large-scale yield surface,  $Y_3$ .

## RÉSUMÉ

Les effets de l'histoire de sollicitation en contraintes de cisaillement sur les caractéristiques de l'écoulement plastique du sable de Toyoura dense sont étudiés. Le comportement dans le plan  $p'$ , a contrainte moyenne effective constante, est caractérisé, plus particulièrement au niveau des petites déformations, en introduisant deux surfaces de charge  $Y_1$  et  $Y_2$  à l'intérieur de la surface de charge classique  $Y_3$ .

## 1 INTRODUCTION

Failure of the ground has been a main concern in construction of structure. However, it has been recognized that we have to consider not only the failure but also the deformation of the ground, because constructions of large size structures and those close to the adjacent buildings have increased. It is very important to estimate the deformation of the ground even at very small strain level.

In conventional yield surface models, which have been used for practice, yield surface is defined at relatively large shear strain, in many cases assuming to coincide with the state boundary surface, and the deformation behavior is assumed elastic within the yield surface. However, actual behavior of soil is non-linear even within that yield point. Elastic behavior of sand is observed only at very small strain of the order of 0.001% (e.g. Kuwano et al., 2001). The deformation behavior beyond this strain level is highly non-linear with rapid decrease in stiffness moduli, that is, the conventional yield surface model does not describe the behavior of sand accurately within the yield surface (e.g. Chaudhary and Kuwano, 2003).

To describe the behavior within the conventional yield surface, Jardine (1992) proposed multiple yield surface model in  $p'$ - $q$  plane. It consists of three yield surfaces  $Y_1$ ,  $Y_2$  and  $Y_3$ . The  $Y_3$  yield locus represents the large-scale yield surface, which is the same as conventional yield surface. The sub-yield surfaces  $Y_1$  and  $Y_2$  are mobile with a stress point. In this study, effects of shear stress history on yielding characteristics of dense Toyoura sand were investigated in  $p'$ -constant shear plane. To characterize the nonlinear features of soil, the multiple yield surface model was adapted to the shear characteristics in  $p'$ -constant shear plane.

## 2 TEST OUTLINE

Hollow cylinder apparatus was used. It gives an advantage over conventional triaxial apparatus as the torsional shear stress can be applied to the specimen in addition to the deviator shear stress as shown in Fig.1. Also three normal stresses can be varied independently, unlike the conventional triaxial apparatus where two normal stresses in radial direction are always equal. Therefore a general stress path of any kind can be applied to the

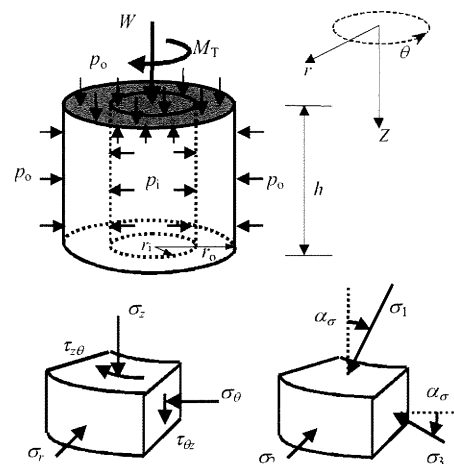


Figure 1. Stress components in hollow cylinder specimen

specimen.

The details of hollow cylinder apparatus used in this study is described in Chaudhary et al. (2002, 2004). Vertical load ( $W$ ) was controlled by air pressure. The torque ( $M_T$ ) was controlled by oil pressure. Inner and outer cell pressures ( $p_i$  and  $p_o$ ) were applied by air pressure controlled by E/P transducer. All the stress and strain measuring devices were connected to amplifier and then to a personal computer through a 16-bit A/D converter. It makes automatic measuring and system control possible.

Toyouura sand specimens were prepared by air pluviation method, to achieve the relative density of 80%. Specimens were saturated by vacuum method, and consolidated isotropically to  $p'=98.1\text{kPa}$  then sheared in drained condition in  $p'$ -constant plane as shown in Fig.2.

Specimens were sheared on  $p'=98.1\text{kPa}$  constant plane. Soil deformation consists of two components, shear and volumetric strains. If  $p'$  is constant, we can observe only effects of shearing. During shearing, the parameter for intermediate principal stress,  $b$ -value, was kept at 0.5. Therefore  $\sigma_2=\sigma_r$  was constant throughout the shearing.

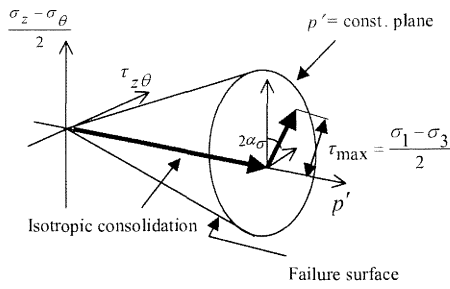


Figure 2. Consolidation and shear stress paths in the test

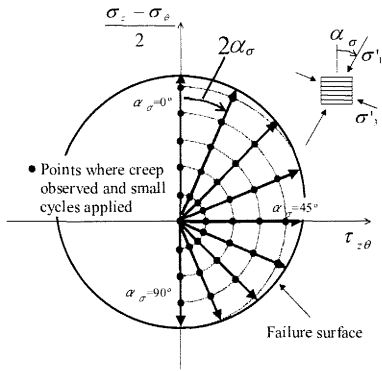


Figure 3. Shear stress path for the test series 1

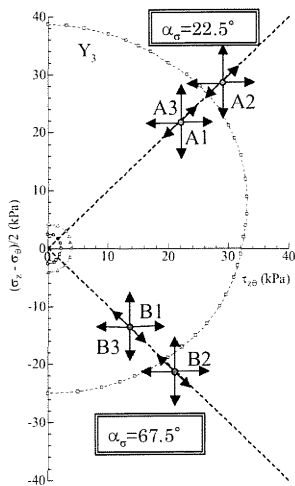


Figure 4. Shear stress paths for the test series 2-7

At various maximum shear stress,  $\tau_{max}$ , during shearing, creep tests were carried out, keeping  $\tau_{max}$  constant for more than 2~3 hours to observe creep characteristics of sand. Then small unload reload cycles of  $\Delta\sigma_z$ ,  $\Delta\sigma_\theta$  and  $\Delta\tau_{z\theta}$  whose magnitude was generally  $\pm 2$  kPa,  $\pm 4$  kPa and  $-6$  kPa, were applied to measure quasi-elastic moduli at various stress states.

Seven series of tests were carried out in this study. In the series 1, nine specimens were isotropically consolidated to  $p'=98.1$  kPa. Then they were sheared along various  $\alpha_\sigma$  directions from the isotropic stress state point as seen in Fig.3. The radial shearing test to study the yield behavior around any stress point is called 'stress probing test'.

In the series 2, six specimens consolidated isotropically were pre-sheared  $\alpha_\sigma=22.5$  deg. to  $\tau_{max}=30$  kPa which is within  $Y_3$  yield surface obtained from test series 1. Then stress probing tests from Point A1 were carried out along six directions. While, in the series 3, 6 specimens were sheared along  $\alpha_\sigma=67.5$  deg. to  $\tau_{max}=20$  kPa, then stress probing tests from B1 were carried out.

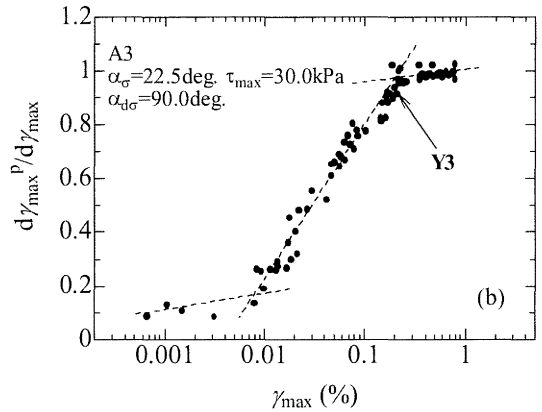
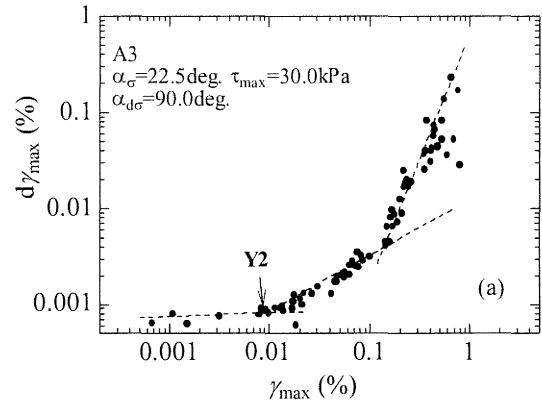


Figure 5. Increase in strain increment with total shear strain

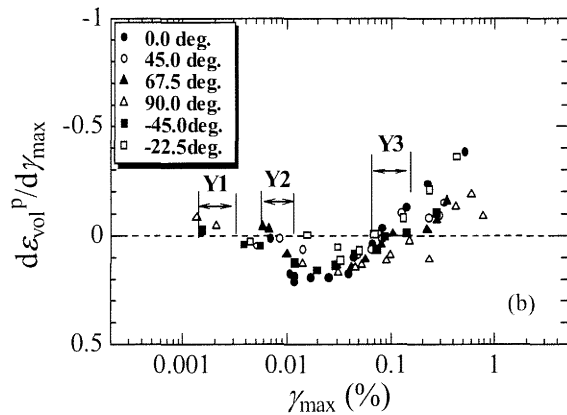
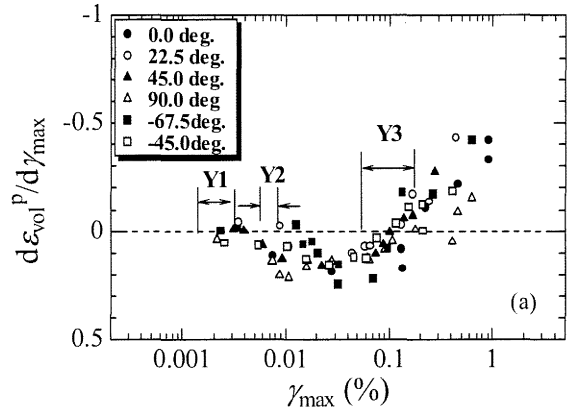


Figure 6. Change in plastic volumetric strain increment ratio with total shear strain. (a) Series 6, (b) Series 7.

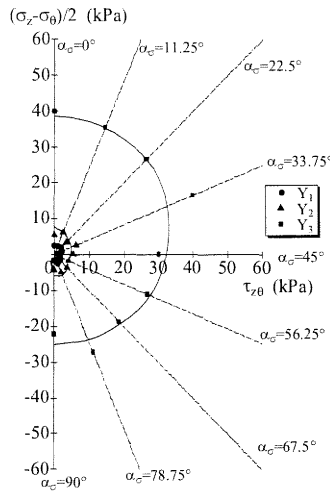


Figure 7.  $Y_1$ ~ $Y_3$  surfaces in series 1

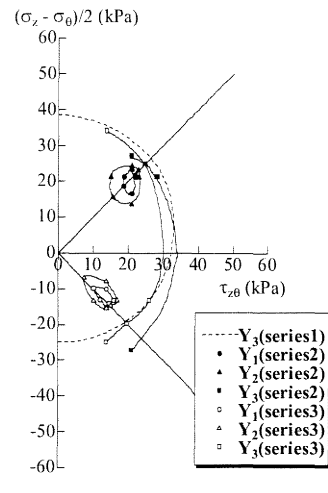


Figure 8.  $Y_1$ ~ $Y_3$  surfaces in series 2 and 3

In the series 4, six specimens consolidated isotropically were pre-sheared along  $\alpha_\sigma = 22.5^\circ$  to  $\tau_{\max} = 39\text{kPa}$  which is outside  $Y_3$  yield surface obtained from the series 1. Then stress probing tests were carried out from A2. While, in the series 5, 6 specimens were sheared along  $\alpha_\sigma = 67.5^\circ$  to  $\tau_{\max} = 30\text{kPa}$ , then stress probing tests from B2 were carried out.

In the series 6, six specimens consolidated isotropically were pre-sheared along  $\alpha_\sigma = 22.5^\circ$  to  $\tau_{\max} = 39\text{kPa}$  which is outside initial  $Y_3$  surface, then unloaded to  $\tau_{\max} = 30\text{kPa}$  along the same direction, and then stress probing tests from A3 were carried out. In the series 7, six specimens consolidated isotropically were pre-sheared along  $\alpha_\sigma = 67.5^\circ$  to  $\tau_{\max} = 30\text{kPa}$ , and unloaded to  $\tau_{\max} = 20\text{kPa}$  then stress probing tests from B3 were carried out.

Stress conditions in the test series 2 to 7 are summarized in Fig.4.

### 3 DETERMINATION OF YIELD POINTS

To describe the nonlinear features of soil, the multiple yield surface model proposed by Jardine (1992) was adapted to the shear characteristics in  $p'$ -constant shear plane. It consists of three yield surfaces  $Y_1$ ,  $Y_2$  and  $Y_3$ . The  $Y_3$  yield locus represents the large-scale yield surface, which is the same as the conventional yield surface. The sub-yield surfaces  $Y_1$  and  $Y_2$  are mobile with a stress point. The  $Y_1$  surface is the linear elastic limit. It is observed in this study that the behavior is linear up to a shear strain of about 0.002%.  $Y_2$  surface represents the commencement of rapid development in plastic strain.

Fig.5 shows (a) the total strain increment,  $d\gamma_{\max}$ , against maximum shear strain,  $\gamma_{\max}$ , relationship, and (b) plastic strain increment ratio,  $d\gamma_{\max}^p/d\gamma_{\max}$ , against  $\gamma_{\max}$ . It is seen that the total strain increment starts to develop rapidly at some point. This point was designated as  $Y_2$ . As seen in Fig.5, both  $d\gamma_{\max}$  and  $d\gamma_{\max}^p/d\gamma_{\max}$  start to increase rapidly with  $\gamma_{\max}$  at a strain level of about 0.01%. Fig.6 shows the plastic volumetric strain increment ratio,  $d\varepsilon_{\text{vol}}^p/d\gamma_{\max}$ , against,  $d\gamma_{\max}$ . It is seen that the plastic volumetric strain starts to be induced at around  $Y_2$  point. It corresponds to the initiation of excess pore pressure generation in undrained shear.

In Fig.5(b), it is also found that the plastic strain increment ratio converged between 0.8 and 1.0. It represents that the sand completely yielded and strain increment became almost plastic in this strain level. The turning point in this relationship was determined as  $Y_3$ . The strain level at  $Y_3$  yield was about 0.1%.

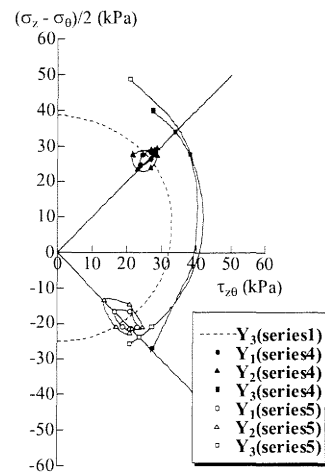


Figure 9.  $Y_1$ ~ $Y_3$  surfaces in series 4 and 5

### 4 YIELD SURFACE

Yield points obtained as above are plotted in  $p'$ -constant plane in Figs.7~10.

The results from the series 1 are summarized in Fig.7. In this test series, tests were not carried out in area of  $\tau_{z\theta} < 0$ , considering yielding character is symmetrical with respect to  $(\sigma_z - \sigma_\theta)/2$  axis. It was observed that  $Y_1$  and  $Y_2$  loci were roughly circular in shape without shifting one-side. It shows little anisotropy in  $Y_1$  and  $Y_2$ . While,  $Y_3$  surface was circular with the center shifted towards compression side ( $(\sigma_z - \sigma_\theta)/2 > 0$ ), that is,  $Y_3$  locus has inherent anisotropy.

The plot of yield loci obtained from the series 2 and 3 are given in Fig.8. In these test series, specimens were pre-sheared within initial  $Y_3$  yield surface. The sub-yield loci  $Y_1$  and  $Y_2$  moved with current stress point and they were now elliptical in shape, compared to the circular shape in the test series 1. They tended to orient along the direction of shearing. It was observed that  $Y_3$  yield loci was approximately at the same place as that from the series 1, that is,  $Y_3$  locus does not move with current stress point within initial  $Y_3$  surface.

The results from the test series 4 and 5 are shown in Fig.9. The same tendency as former series was obtained about  $Y_1$  and  $Y_2$  loci, moving with current stress point and being elliptical in

shape orienting along the direction of shearing. On the other hand,  $Y_3$  has grown in size and moved outward from the initial  $Y_3$  surface. This indicates that the  $Y_3$  surface is modified when it is intersected by the current stress point, and is not affected when the stress point is within the initial  $Y_3$  surface. This may be considered as hardening of conventional yield surface.

The results from the test series 6 and 7 are shown in Fig.10. Like former series,  $Y_1$  and  $Y_2$  moved with the current stress point and were elliptical in shape and oriented along the direction of shearing. Regarding the size, however, different tendency was observed.  $Y_1$  was the same in size as the other test series, while the size of  $Y_2$  has grown by load-unload shear stress history. In these test series, the shearing was made up to  $\tau_{z\theta} < 0$  region and  $Y_3$  yield surface was drawn as closed curve. It can be seen that  $Y_3$  locus was still symmetric with respect to  $(\sigma_z - \sigma_\theta)/2$  axis. Their sizes were approximately the same as extended  $Y_3$  surface, or little bit smaller than that. This indicates that  $Y_3$  yield surface shows isotropic hardening by loading, but not softening by unloading.

In Fig.10, plastic strain increment vectors are also shown. Both stress and strain are shown in the same plane. The vectors show only the direction of plastic increment, not magnitude. It can be seen that the plastic strain increment vectors are normal to  $Y_3$  yield surface while not to  $Y_2$ . This indicates that  $Y_3$  yield surface and plastic potential coincide with each other, that is, associated flow rule.

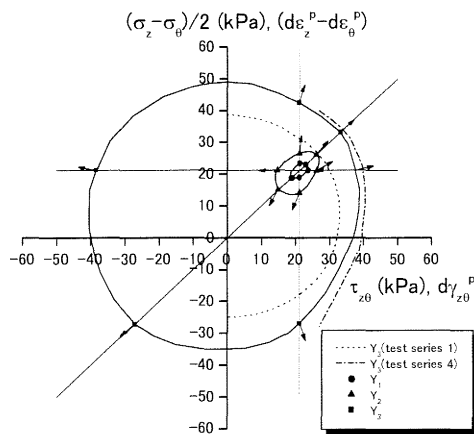


Figure 10(a).  $Y_1 \sim Y_3$  surfaces in series 6

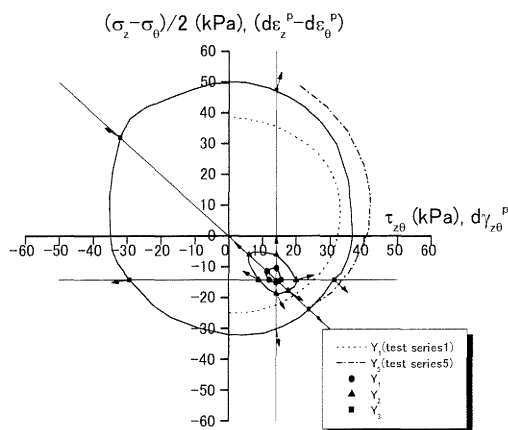


Figure 10(b).  $Y_1 \sim Y_3$  surfaces in series 7

## 5 CONCLUSIONS

The yielding behavior was characterized, especially at very small strain level, by introducing two sub yield surfaces  $Y_1$  and  $Y_2$  inside the conventional large-scale yield surface,  $Y_3$ . The characteristics of these three yield surfaces were obtained as follows:

1.  $Y_1$  yield surface is mobile with current stress state point. It changes the shape into elliptical as it moves to anisotropic stress state. Its size does not change.

2. Like  $Y_1$  yield surface,  $Y_2$  yield surface is mobile with the current stress state point and changes the shape into elliptical as it moves to anisotropic stress state. It becomes larger after the loading-unloading stress history.

3.  $Y_3$  yield surface is comparatively immobile. It stays around the isotropic stress state point. It becomes larger when it is intersected by the current stress point. It shows isotropic hardening.

4. The direction of the plastic shear strain increment vector is not normal to  $Y_2$ , but it becomes normal to  $Y_3$  for the further shearing. Therefore, associated flow rule can be applied to  $Y_3$ .

## REFERENCES

- Chaudhary, S.K., and Kuwano, J. 2003. Anisotropic multiple yielding of dense Toyoura sand in  $p'$ -constant shear plane. *Soils and Foundations*, 43 (4), 59-69.
- Chaudhary, S.K., Kuwano, J., Hashimoto, S., Hayano, Y. and Nakamura, Y. 2002. Effects of initial fabric and shearing direction on cyclic deformation characteristics of sand. *Soils and Foundations*, 42 (1), 147-157.
- Chaudhary, S.K., Kuwano, J. and Hayano, Y. 2004. Measurement of quasi-elastic stiffness parameters of dense Toyoura sand in hollow cylinder apparatus and triaxial apparatus with bender elements. *Geotechnical Testing Journal*, 27 (1), 23-35.
- Jardine, R.J. 1992. Some observations on the kinematic nature of soil stiffness. *Soils and Foundations*, 32 (2), 111-124.
- Kuwano, J., Hashimoto, S. and Chaudhary, S.K. 2001. Shear stress dependency of small-strain stiffness and creep of Toyoura sand. *Proceedings of 15th International Conference on Soil Mechanics and Geotechnical Engineering*, Istanbul, 179-182.